

# **<sup>1</sup>H NMR characterization of renatured lysozyme obtained from fully reduced lysozyme under folding/oxidation conditions: a high-resolution liquid NMR study at magic angle spinning**

Muriel Delepierre,<sup>1\*</sup> Pascale Roux,<sup>2</sup> Alain-F. Chaffotte<sup>2</sup> and Michel E. Goldberg<sup>2</sup>

<sup>1</sup> Laboratoire de RMN, CNRS URA 1129, Institut Pasteur, 28 rue du Dr Roux, 75724 Paris Cedex 15, France

<sup>2</sup> Unité de Biochimie Cellulaire, CNRS URA 1129, Institut Pasteur, 28 rue du Dr Roux, 75724 Paris Cedex 15, France

Received 2 February 1998; revised 2 April 1998; accepted 3 April 1998

**ABSTRACT:** Magic angle spinning (MAS) has long been used as a powerful technique in studies of heterogeneous samples such as powdered solids, compartmentalized liquids and heterogeneous solid–liquid mixtures. Recently it has been shown that higher resolution could be achieved if high-resolution magnetic susceptibility matching probe technology was used in conjunction with MAS (Nano-probe). In this paper the possibilities and advantages of generating high-resolution spectra of liquids is illustrated using the Nano.nmr probe for the study in solution of lysozyme subjected to various treatments. © John Wiley & Sons Ltd.

**KEYWORDS:** NMR; <sup>1</sup>H NMR; magic angle spinning; small volume sample; lysozyme

## **INTRODUCTION**

In order to investigate further the role of the disulfide bridges in the folding process of lysozyme, the complete refolding of reduced lysozyme has been studied using conditions under which the aggregation of lysozyme was minimized.<sup>1</sup> It has been shown previously that when the native disulfide bonds are maintained in the denatured state, the protein recovers the majority of its secondary structure in less than 4 ms,<sup>2</sup> while, after this time of renaturation, the reduced protein remained fully unfolded. In the reduced form, the species that are present after 4 ms of refolding have a random coil circulation dichroism (CD) signal in the far-UV region.<sup>3</sup> However, the reduced lysozyme is able slowly to recover its native structure when the disulfides bonds are allowed to form.<sup>4</sup> Therefore, it appeared that the disulfide bridges accelerate the acquisition of the secondary structure or stabilize it in very early stages of the folding process. This raised the question of whether the formation of the secondary structure brings together the cysteines in the proper conformation to form native disulfide bonds, or whether the disulfide bridges are formed first, thereby inducing the formation of secondary structure?

The answer to the question of the role of the disulfide bridges can be examined through comparative studies

of the kinetics of re-establishment of both secondary structure and disulfide bonds during the oxidative folding of the reduced wild-type lysozyme and of mutant lysozyme missing some of the cysteine pairs. The kinetics of far-UV CD, intrinsic fluorescence and enzymatic activity recovery<sup>1</sup> have already shown that during oxidative folding of reduced lysozyme, regaining activity and acquisition of the secondary structure are strongly coupled during the whole folding process. Under such conditions, it was shown that the renatured egg hen white lysozyme (HEWL) is fully native. Indeed, the renatured lysozyme could not be distinguished from native lysozyme according to the following criteria: similar specific activity, same compactness, superimposable CD and fluorescence spectra, same mass, same thermodynamic stability and identical proton NMR spectra.

To characterize further and understand the folding process, it is important to determine whether only native disulfide bonds are effective in promoting secondary structure elements, thus allowing us to probe the influence of specific long-range interactions on the early stages of the folding process. Moreover, in all cases it is important to show that the renatured lysozyme is identical with the native protein and to analyze, from a structural point of view, the mutant lysozymes missing some of the cysteine pairs.

Experiments with reduced lysozyme are difficult as renaturation often leads to aggregation states. However, a buffer system that leads to a low percentage of aggregation has been described.<sup>1</sup> Although the conditions were optimized, physico-chemical analysis of the protein obtained would require a lot of material, especially for NMR measurements. Hence it was of great interest to

\* Correspondence to: M. Delepierre, Laboratoire de RMN, CNRS URA 1129, Institut Pasteur, 28 rue du Dr Roux, 75724 Paris Cedex 15, France.

E-mail: muriel@pasteur.fr

Contract/grant sponsor: Institut Pasteur.

Contract/grant sponsor: Centre National de la Recherche Scientifique (URA 1129).

be able to achieve such NMR studies with very small quantities of compound. We have previously shown that using Nano-nmr probe technology one can obtain high-quality spectra for volumes as small as 40  $\mu\text{l}$ .<sup>1,5,6</sup> In this paper, we show that this new technology can be applied efficiently to protein molecules at concentrations similar to those used with conventional 5 mm probes (650  $\mu\text{l}$ ), resulting in a reduction of 15–100-fold in the amount of material needed. In addition, we show that standard 2D experiments such as TOCSY and NOESY can be achieved efficiently under these conditions.

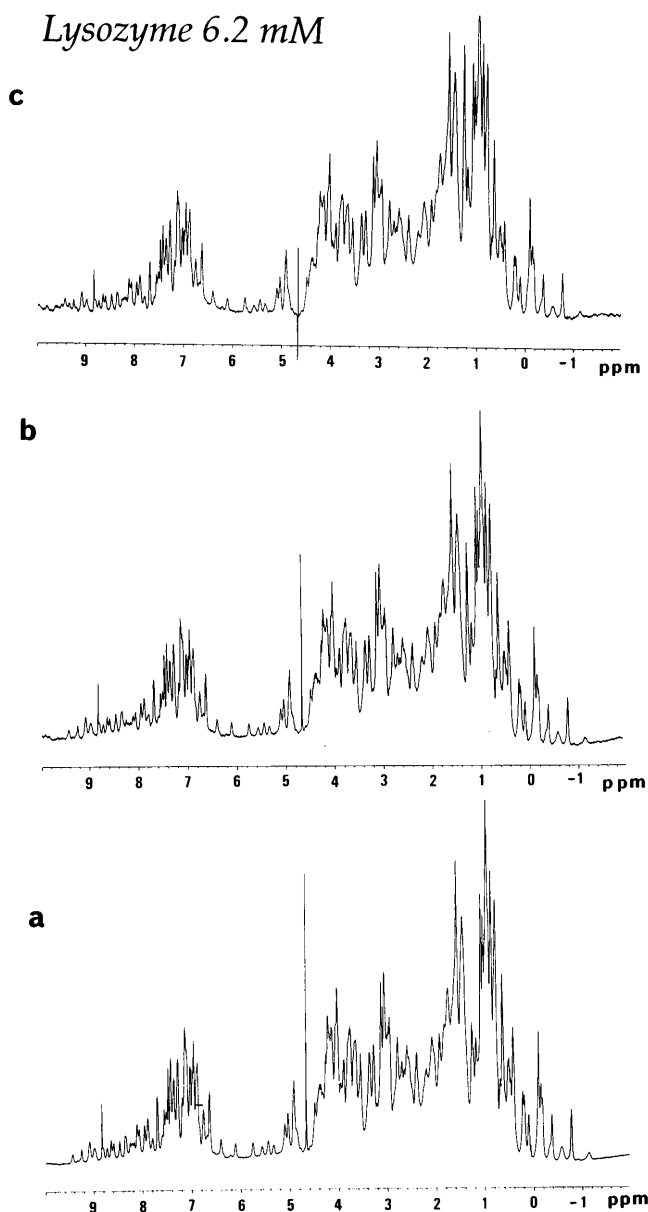


**Figure 1.** One-dimensional proton NMR spectra of native lysozyme, 6.2 mM in  $\text{D}_2\text{O}$ , acquired at 25 °C with 32 scans with strictly identical shim settings. Spinning rate, 2240 Hz. (a) 40  $\mu\text{l}$ , corresponding to 27  $\mu\text{mol}$ ; (b) 20  $\mu\text{l}$ , corresponding to 13  $\mu\text{mol}$ ; (c) about 6  $\mu\text{l}$ , corresponding to 50 nmol.

## EXPERIMENTAL

### Sample Preparation

Hen egg white lysozyme was obtained from Boehringer Mannheim (Mannheim, Germany). Three different samples were used for the NMR experiments: one corresponding to the native lysozyme, one corresponding to the native lysozyme subjected to incubation in the renaturing buffer and one corresponding to the renatured lysozyme sample. The composition of the renaturation buffer was 0.5 M guanidium chloride, 60  $\mu\text{M}$  oxidized glutathione and 20  $\mu\text{M}$  reduced dithiothreitol in which aggregation of lysozyme was minimized and where a renaturation yield of 80% was obtained.<sup>1</sup> All the samples were dialyzed extensively at pH 3 before use and freeze-dried. The reduced/denatured hen egg white lysozyme was prepared as described by Goldberg *et al.*<sup>7</sup> Briefly, protein solution (20 mg  $\text{m}^{-1}$ ) in 0.1 M Tris-HCl (pH 8.6) containing 10 M urea and 0.15 M DTT was incubated at room temperature for 2 h. The solution was then acidified to pH 3 by addition of HCl, dialyzed extensively against 0.1 M deuterated acetic acid at 4 °C and then lyophilized. The lyophilized powders were dissolved in 40  $\mu\text{l}$  of  $\text{D}_2\text{O}$  (Euriso-Top) or deuterated acetic acid (0.1 M)- $\text{D}_2\text{O}$  for the reduced lysozyme. The lysozyme concentration, determined by measuring from the UV absorbance at 280 nm, was 6.2 mM for the native lysozyme, 0.9 mM for the native lysozyme incubated in the renaturing buffer and 2.8 mM for both the renatured lysozyme and the reduced/denatured lysozyme.

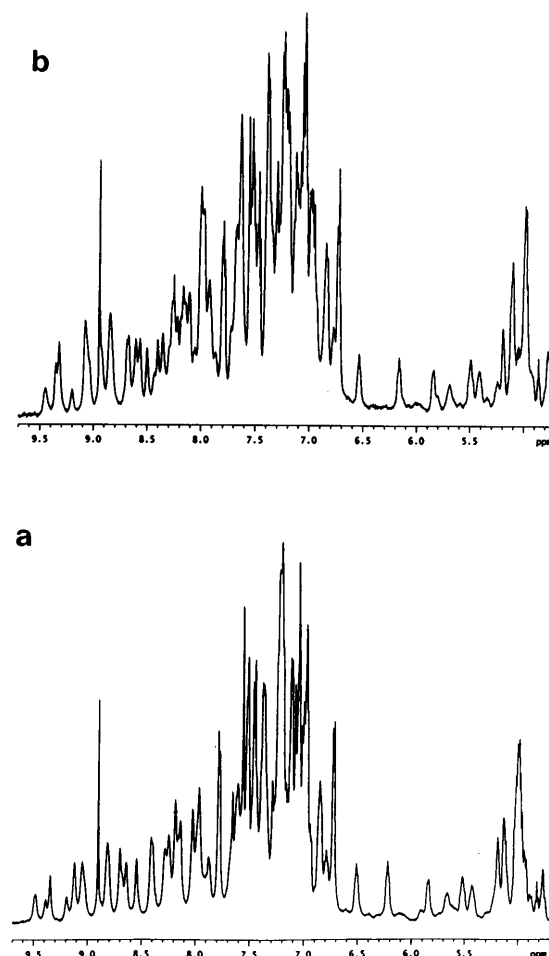


**Figure 2.** Low-field region of the one-dimensional proton NMR spectra of lysozyme. (a) Native lysozyme; (b) renatured lysozyme.

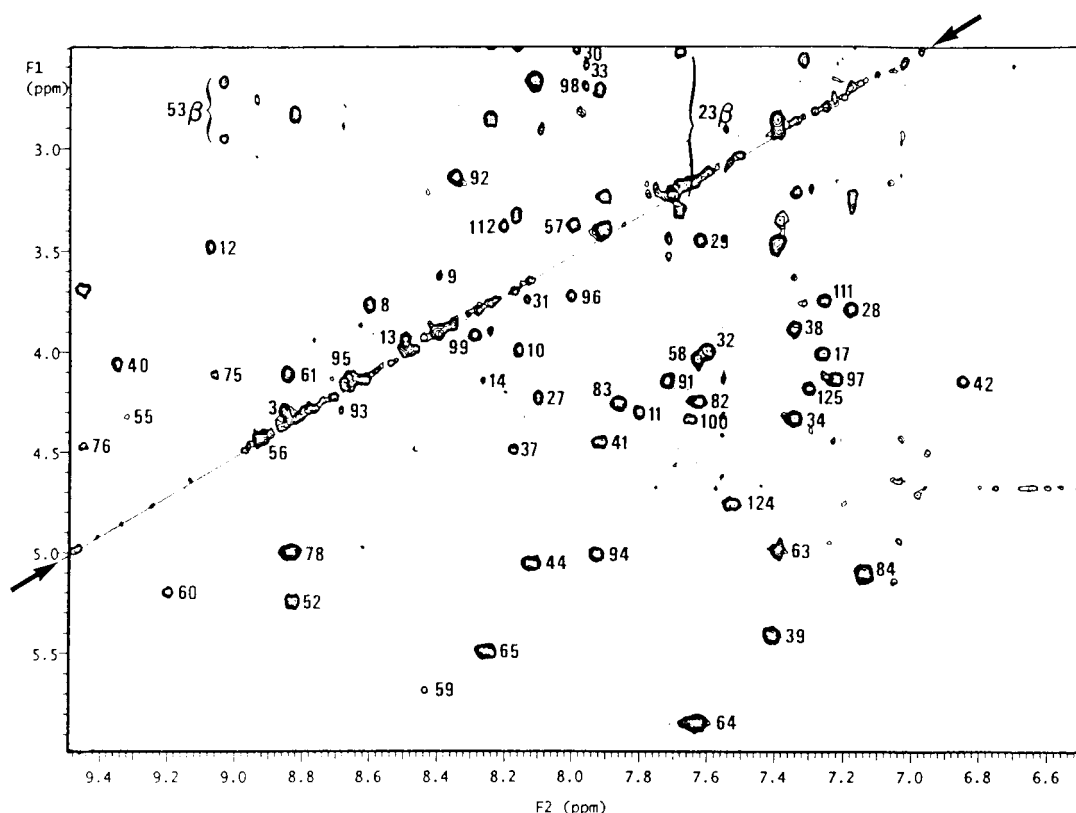


**Figure 3.** Contour plot of a TOCSY spectrum of renatured lysozyme at 2.8 mm obtained at 35 °C in  $\text{D}_2\text{O}$ . Spin systems are labelled with the sequential residue position. Artefacts due to the spinning side bands are shown in the spectrum with two arrows.

### $^1\text{H}$ NMR experiments

$^1\text{H}$  NMR experiments, using a Nano-nmr probe (Varian, Palo Alto, CA, USA), were run at 500 MHz on a Varian Unity spectrometer with an on-line Sun Sparc 2 workstation. The 90° pulse was set at 11.1  $\mu\text{s}$  using about half the power required for the same pulse width with our standard 5 mm probe. The experimental data were processed using the VNMR 5.1B program. The spectral width was 7200 Hz and the spinning rate around 2 kHz  $\pm$  10 Hz. Spectra were referred to the water signal at 4.68 ppm at 35 °C and 4.78 ppm at 25 °C [relative to 3-trimethylsilyl-(2,2,3,3- $^2\text{H}_4$ ) propionate (TMSP), the external reference]. Quadrature detection was employed in all experiments with the carrier frequency always maintained at the solvent resonance. The two-dimensional  $^1\text{H}$  NMR spectra were recorded in the phase-sensitive mode<sup>8</sup> with 3200 data points in the  $t_2$  dimension and 440  $t_1$  increments; 8–16 scans were acquired for the TOCSY (total correlated spectroscopy) experiment with a mixing time of 60 ms, giving a total acquisition time of about 3–7 h, and 8, 32, 48 or 64 scans for the NOESY (nuclear Overhauser effects spectroscopy) experiments, depending on the concentration, with a single mixing time of 150 ms to allow direct comparison with previously published data,<sup>9</sup> giving a total acquisition time of about 5–36 h. Zero-filling was applied prior to Fourier transformation and data were processed with shifted sine-bell window functions in

both dimensions. Low-power selective irradiation during the recycling delay and, for NOESY spectra, during the mixing period was used to suppress the residual water peak.

### RESULTS AND DISCUSSION

The Nano-probe produces high-resolution spectra in sample volumes of about 40  $\mu\text{l}$  or less<sup>10</sup> at concentrations similar to those used with standard 5 mm probes. This is obtained as a result of high-resolution magnetic susceptibility matching probe technology used in conjunction with magic angle spinning.<sup>11</sup> Magnetic susceptibility broadening due to the use of non-spherical samples is efficiently removed by spinning the sample at the magic angle, which allows the collection of spectra with sample volumes from 5 to 40  $\mu\text{l}$  with an identical shim setting (Fig. 1). The probe uses a solenoidal coil to maximize the available sensitivity,<sup>12</sup> which is placed immediately around the sample, giving a very good filling factor. In addition, high detection efficiency is obtained by placing 100% of the sample in the receiver coil.<sup>13,14</sup> A signal-to-noise ratio (S/N) of 106 was obtained with the standard test sample of 0.1% ethylbenzene in deuterated chloroform. This value can be compared with the S/N of 400 obtained on our 8-year-old spectrometer under the same conditions with a stan-

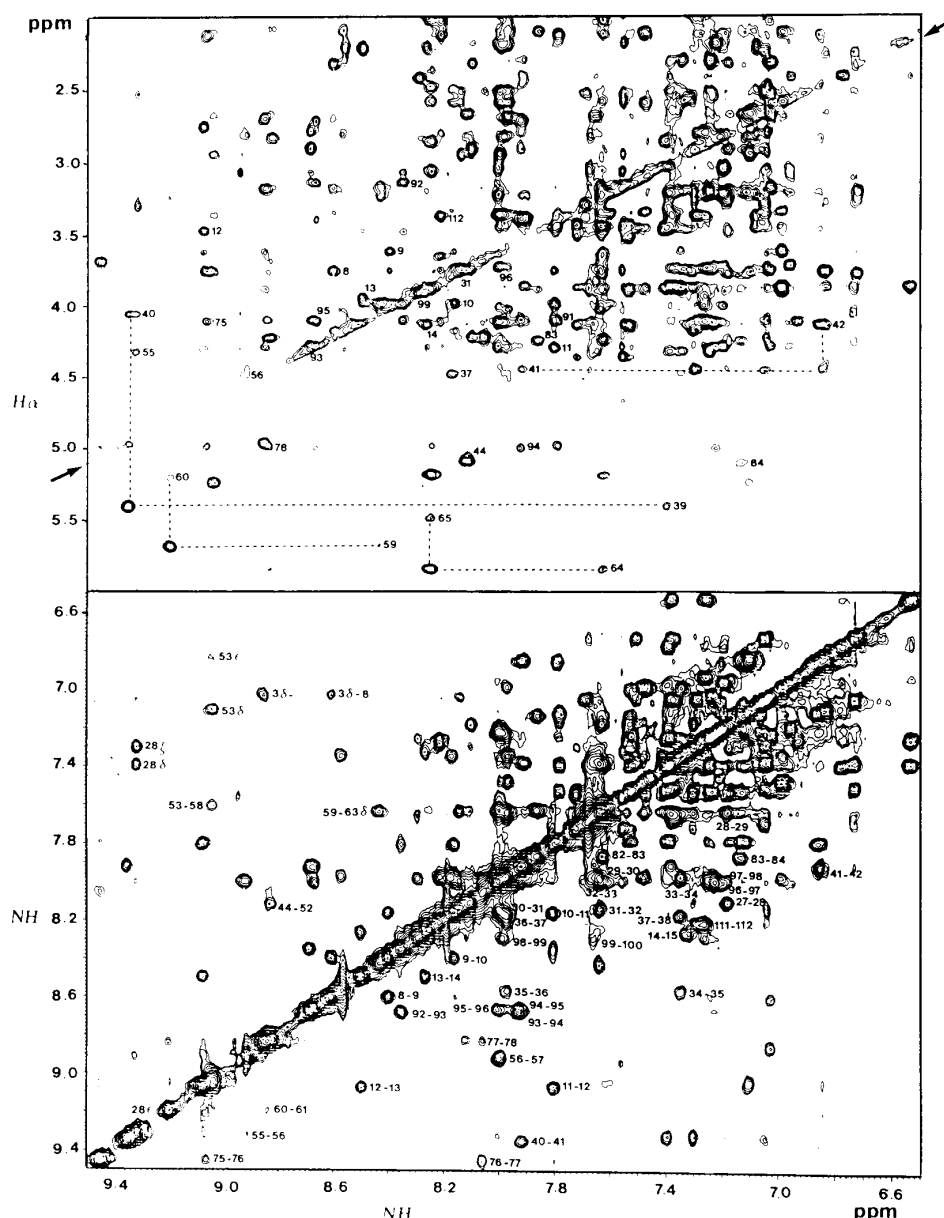


**Figure 4.** NOESY spectrum of renatured lysozyme at 2.8 mm recorded with a 150 ms mixing time at 35 °C. Top, contour plot of the NH, H $\alpha$  region. The  $d_{\alpha N}$  sequential connectivities are indicated. Bottom, contour plot of the amide region. Connectivities involving pairs of neighboring amide protons are labeled in the region below the diagonal and long-range interactions are labeled in the region above the diagonal. Artefacts due to the spinning side bands are shown in the spectrum with two arrows.

standard 5 mm probe. Obviously modern 5 mm probes have an S/N larger than 400 but the comparison is still valid when the sample amount is limited. Assuming that, in standard geometry probe, about one third of the sample resides within the active region of the receiver coil, that is about 220  $\mu$ l, a ratio of only 4 is obtained for the S/N if the standard probe is to be compared with the Nano-probe while the volume ratio is 5.5:1 in favor of the Nano-probe when ratioing the active volume of the 5 mm probe (220  $\mu$ l) to the total volume of the Nano-cell which is all active. If we now compare the overall sample volume of a standard 5 mm probe, a ratio of 16.2:1 is obtained. To complete these comparisons, an S/N test was also performed with a Shigemitsu 5 mm micro cell and a value of 400 was also obtained.

However, the counterpart of this is that because the sample is spinning during the entire experiment, spinning side bands may be obtained in the spectra and in all dimensions of multi-dimensional experiments. These artefacts appear as spurious cross peaks aligned parallel to the diagonal. The inconvenience of this can be easily overcome by changing the spinning rate or the temperature. Rotor synchronization with pulse sequence, similarly to that used for solid-state experiments, helps but a lot of evaluation still needs to be done.

The spectra obtained in D<sub>2</sub>O for the three samples, that is, native lysozyme, native lysozyme incubated in the renaturing buffer and renatured lysozyme, exhibit similar features (Fig. 2). The TOCSY maps obtained for the native lysozyme together with the known assign-

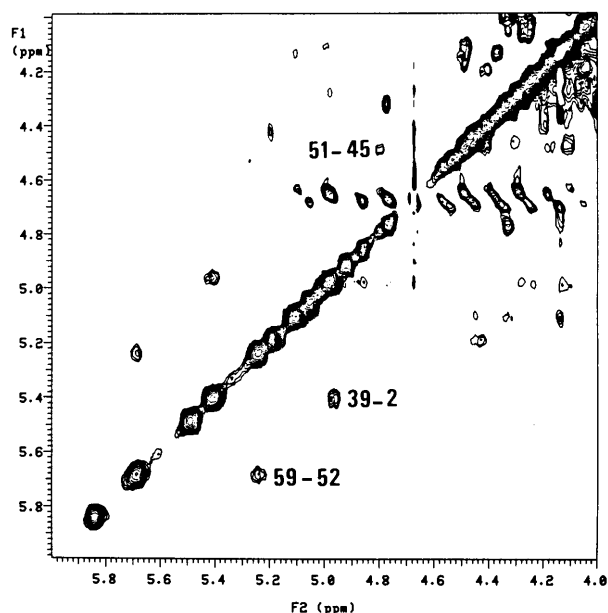


**Figure 5.** Part of the NOESY spectrum of the renatured lysozyme showing long-range  $d_{\alpha\alpha}$  connectivities characteristic of antiparallel  $\beta$ -sheet structures.

ments for the native lysozyme<sup>9</sup> allowed us to assign 63 amide protons in the renatured lysozyme. The fingerprint region (NH, H $\alpha$ ) of the renatured lysozyme spectrum contains 57 NH-H $\alpha$  cross peaks while six NHs, namely Tyr23, Glu35, Ser36, Tyr53, Trp108 and Cys115, exhibit cross peaks with  $\beta$ -protons but not with their H- $\alpha$  proton, confirming their presence (Fig. 3). Several explanations can account for this. First, the H $\alpha$  proton can be bleached out during the presaturation of the water signal (Trp108, for example). Alternatively, the  $^3J_{\text{NH}, \text{H}\alpha}$  coupling constant may be too small for efficient transfer or the use of a unique mixing time for the isotropic mixing may be unfavorable. These results are in fair agreement with the 64 amide protons shown to exchange slowly (58) or at an intermediate rate (6).<sup>8</sup> As reported previously, exchange rates correlate with elements of secondary structure present in the protein.<sup>9,15-17</sup> The  $d_{\text{NN}}$  and  $d_{\alpha\text{N}}$  connectivities identified in the NOESY spectra are shown in Fig. 4 for the renatured lysozyme. Thus, extended regions of  $d_{\text{NN}}$  connectivities are observed for residues 8-14/15, 27-38 and 92-100, in agreement with the presence of regular  $\alpha$ -helices. Shorter stretches of  $d_{\text{NN}}$  connectivities are also observed for residues 40-42, 55-57, 75-78, 82-84, 111-112 and 123-125. These regions correspond either to non-regular helices or tight turns. Extended regions of  $d_{\alpha\text{N}}$  sequential connectivities are observed for residues 42-47, 50-55 and 57-60, in agreement with the presence of triple-stranded antiparallel  $\beta$ -sheets. This element of secondary structure is confirmed by several long-range interstrand  $d_{\text{NN}}$  connectivities (44, 52 and 53, 58) (Fig. 4) but also  $d_{\alpha\alpha}$  connectivities (45, 51 and 52, 59) (Fig. 5). Finally, the long-range  $d_{\alpha\alpha}$  interaction (2, 39) (Fig. 4) confirms the short antiparallel  $\beta$ -sheet between residues 2-4 and 39-40. Despite the fact that spectra in Fig. 2 display great similarity, small shifts are observed in the 2D maps (TOCSY and NOESY) for some of the resi-

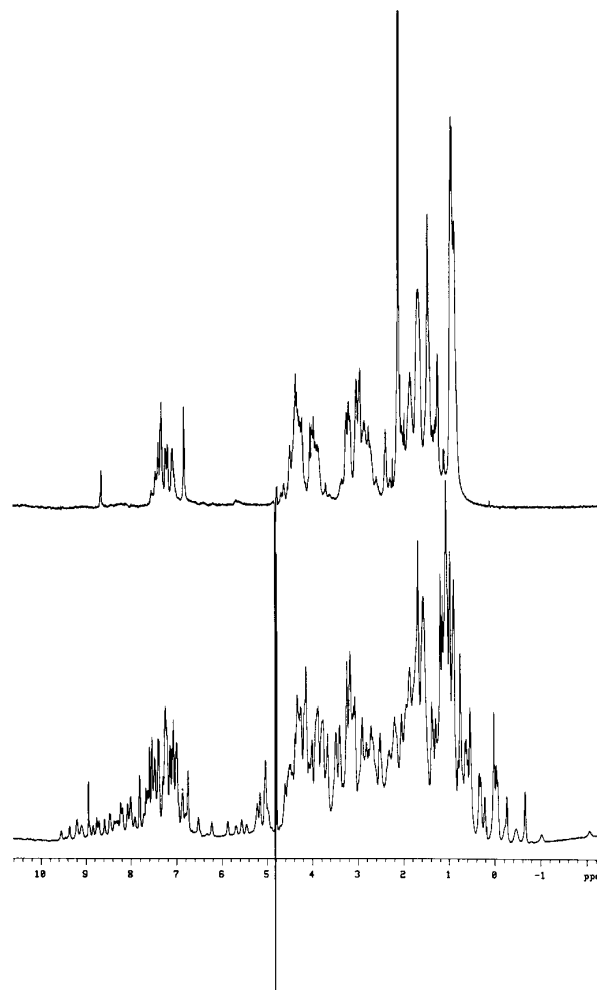


**Figure 6.** One-dimensional proton spectra of lysozyme in  $\text{D}_2\text{O}$  acquired at 25 °C with 32 scans. Spinning rate, 2240 Hz. Bottom, native lysozyme, 6.2 mm; top, reduced/denatured lysozyme, 2.8 mm.

dues. Although the reason for this is unknown, these shifts are also observed when comparing the two native lysozyme samples, that is, the one just dialyzed and the one that had been incubated in the renaturing buffer. A simple explanation is that these small differences are due to components present in the buffer. Indeed, the most perturbed shifts are observed for the  $\beta$ -protons of Asn59, a residue involved in the  $\beta$ -sheet structure and facing the Asp52 residue that is the catalytic residue. Leu17, Thr43, Thr51, Tyr53 and Ile55 resonances are also perturbed but to a lesser extent. The renaturation buffer contains several components, including acetate ions and EDTA. We have already shown that acetate can compete with one of the lanthanide ion binding sites (Asp52 and Glu35) but also that EDTA can bind to lysozyme.<sup>15</sup> This hypothesis is strengthened by the fact that when the native lysozyme sample, subjected to the renaturation buffer, is further dialyzed against water at pH 3, the shifts observed tend to diminish. Indeed, the Asn59  $\beta$ -protons that are separated by 0.04 ppm in the spectrum of the renatured lysozyme and of the native lysozyme incubated in the renaturing buffer are separated by 0.3 ppm in the native lysozyme. When the lysozyme sample incubated in the renaturation buffer is

further dialyzed against water at pH 3 these chemical shift differences decrease from 0.3 to 0.1 ppm.

The spectrum of the reduced lysozyme is shown Fig. 6. There is no significant dispersion in chemical shifts, indicating the absence of a tightly packed hydrophobic core and of strong side-chain interactions. Furthermore, the chemical shift values obtained from the TOCSY experiment (data not shown) for each residue type are very similar to the values predicted for a random coiled structure.<sup>18</sup> Finally, no line broadening effect could be evidenced, excluding the presence of early structural folding intermediate.<sup>19,20</sup> All these observations are in agreement with the absence of secondary structure in reduced lysozyme<sup>1,3</sup> and, of course, with the fact that the disulfide bridges are critical in the folding process. Having set these experimental conditions, it is now possible to investigate the role of the disulfide bridges during the oxidative folding of reduced lysozyme and/or mutant lysozyme missing some of the cysteine pairs.

## CONCLUSION

We have shown that it is possible to collect high-quality spectra in terms of resolution, sensitivity and lineshape with small amounts of product using the Nano.nmr probe. Furthermore, the high detection efficiency achieved by the Nano-probe allows us to obtain spectra with nanomoles of compounds, here 50 nmol for lysozyme, rendering this technique promising when sample quantity is a real limitation. Although the current version of the Nano.nmr probe is available only for proton detection, an inverse detection/gradient version is under development that would allow one to achieve standard heteronuclear experiments. Reduction of the sample size can be seen as a complementary alternative<sup>21,22</sup> to the development of ultra-high-field spectrometers.

## Acknowledgements

The authors acknowledge financial support by the Institut Pasteur and the Centre National de la Recherche Scientifique (URA 1129). We thank the Varian teams at Darmstadt and Paris, Dr Simone Mergui and Vincent Ronfle, for lending the probe and Dr Paul Kiefer of Varian at Palo Alto for stimulating discussions.

## REFERENCES

1. P. Roux, M. Delepierre, M. E. Goldberg and A.-F. Chaffotte, *J. Biol. Chem.* **272**, 24843 (1997).
2. A.-F. Chaffotte, Y. Guillou and M. E. Goldberg, *Biochemistry* **31**, 9694 (1992).
3. M. E. Goldberg and Y. Guillou, *Protein Sci.* **3**, 883 (1994).
4. V. P. Saxena and D. B. Wetlaufer, *Biochemistry* **9**, 5015 (1970).
5. M. Delepierre, A. Prochnika-Chalufour and L. D. Possani, *Biochemistry* **36**, 2649 (1997).
6. M. Delepierre, *J. Chim. Phys.* **95**, 235 (1998).
7. M. E. Goldberg, R. Rudolph and R. Jaenicke, *Biochemistry* **30**, 2790 (1991).
8. D. J. States, R. A. Haberkorn and D. J. Rubens, *J. Magn. Reson.* **48**, 286 (1982).
9. C. Redfield and C. M. Dobson, *Biochemistry* **27**, 122 (1988).
10. A. Manzi, P. V. Salimath, R. C. Spiro, P. A. J. Keifer and H. H. Freeze, *J. Biol. Chem.* **270**, 9154 (1995).
11. W. L. Fitch, G. Detre, C. M. Holmes, J. N. Shoolery and P. A. J. Keifer, *Org. Chem.* **59**, 7955 (1994).
12. D. Hoult and R. E. Richards, *J. Magn. Reson.* **24**, 71 (1976).
13. P. A. J. Keifer, L. Baltusis, D. M. Rice, A. A. Tymiak and J. N. Shoolery, *J. Magn. Reson. A* **119**, 65 (1996).
14. P. A. J. Keifer, *Drug Discovery* in press.
15. M. Delepierre, Thèse d'Etat, Université de Paris Sud (1983).
16. M. Delepierre, C. M. Dobson and F. M. Poulsen, *Biochemistry* **21**, 4756 (1982).
17. M. Delepierre, C. M. Dobson, M. A. Howarth and F. M. Poulsen, *Eur. J. Biochem.* **145**, 389 (1984).
18. A. Bundi and K. Wüthrich, *Biopolymers* **18**, 285 (1979).
19. A.-F. Chaffotte, Y. Guillou, M. Delepierre, H. Hinz and M. E. Goldberg, *Biochemistry* **30**, 8067 (1991).
20. J. I. Guijarro, M. Jackson, A.-F. Chaffotte, M. Delepierre, H. H. Mantsch and M. E. Goldberg, *Biochemistry* **34**, 2998 (1995).
21. D. L. Olson, T. L. Peck, A. G., Webb, R. L. Magin and J. V. Sweedler, *Science* **270**, 167 (1995).
22. D. L. Olson, M. E. Lacey and J. V. Sweedler, *Anal. Chem.* **70**, 645 (1998).